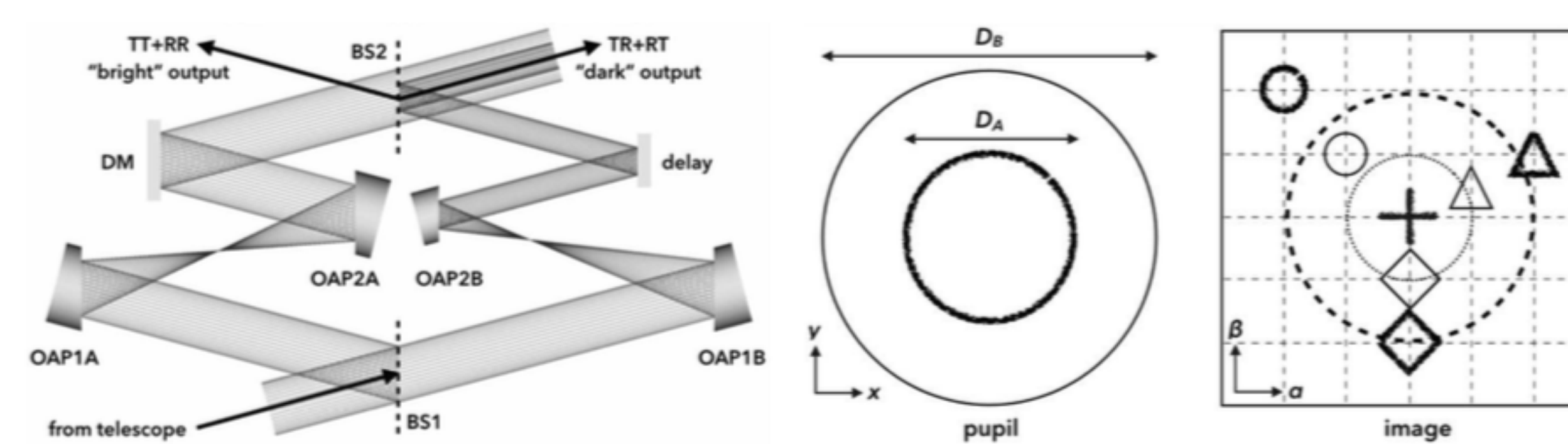


Introduction

One of the biggest goals of astronomy is to discover new planets that could be habitable for life as we know it or otherwise. In order to find habitable candidates, we must search for planets outside of our Solar System, otherwise known as *exoplanets*.

Typical exoplanet and host-star contrasts scale on the order of a billion to one, making them impossible to detect without controlling diffracted and scattered starlight. A next-generation Visible Nulling Coronagraph is being developed using radial shear interferometry to suppress starlight with the goal of enabling exoplanet direct imaging with maximal throughput and discovery space.

Radial Shear Nulling Coronagraph (RSNC)



The principle of operation of the RSNC. *Left*: the RSNC is a radial shearing interferometer that splits light into a reflected "A" arm and transmitted "B" arm of differing magnification that gives rise to circular off-axis transmission. *Right*: resultant pupil and image plane illustrating the difference in magnification. Magnification is shown at 2:1 in the layout and schematics to exaggerate the need for irradiance balancing as well as illustrating the increasingly separated image centers (circles and triangles) for off-axis sources corresponding to decreasingly coherent tilted wavefronts.

Fig. 1: Principle of operation of the RSNC

The optomechanical design of a radial shear nulling coronagraph (RSNC) has been developed to ensure obstruction-free optical propagation and mechanical fit of actuators necessary for mounting and alignment in all required degrees of freedom.

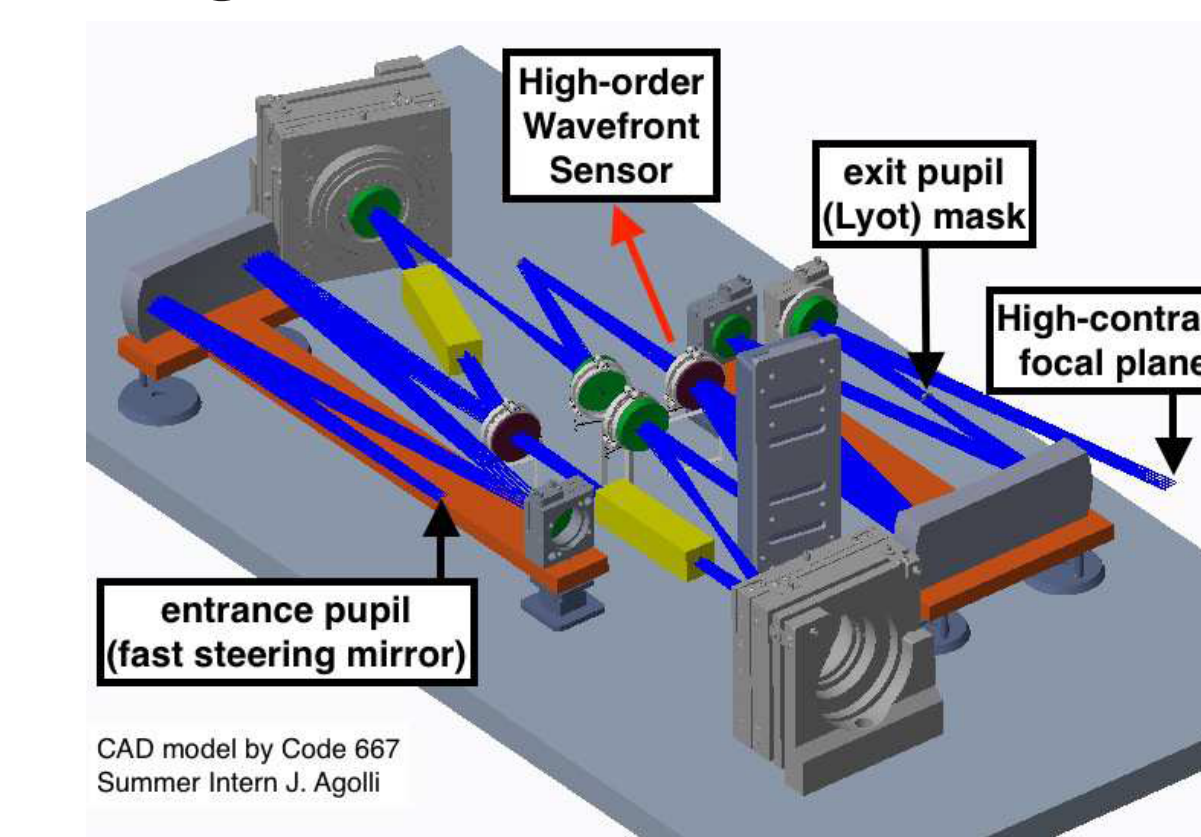


Fig. 2: The initial model of the Radial Shear Nulling Coronagraph, including: **optic beamsplitter**, **mirrors**, **achromatic phase shifters**, and **platforms** allowing for independent alignment.

Kinematic Mounts

Kinematic mounts are used in optical assemblies to enable better stability and repeatability for the relative positioning of components. This is achieved by using the precise number of contact points needed to fully constrain, but not overconstrain, the required degrees of freedom. Repeatability allows the top plates of the T-shaped mounts to be aligned independently.

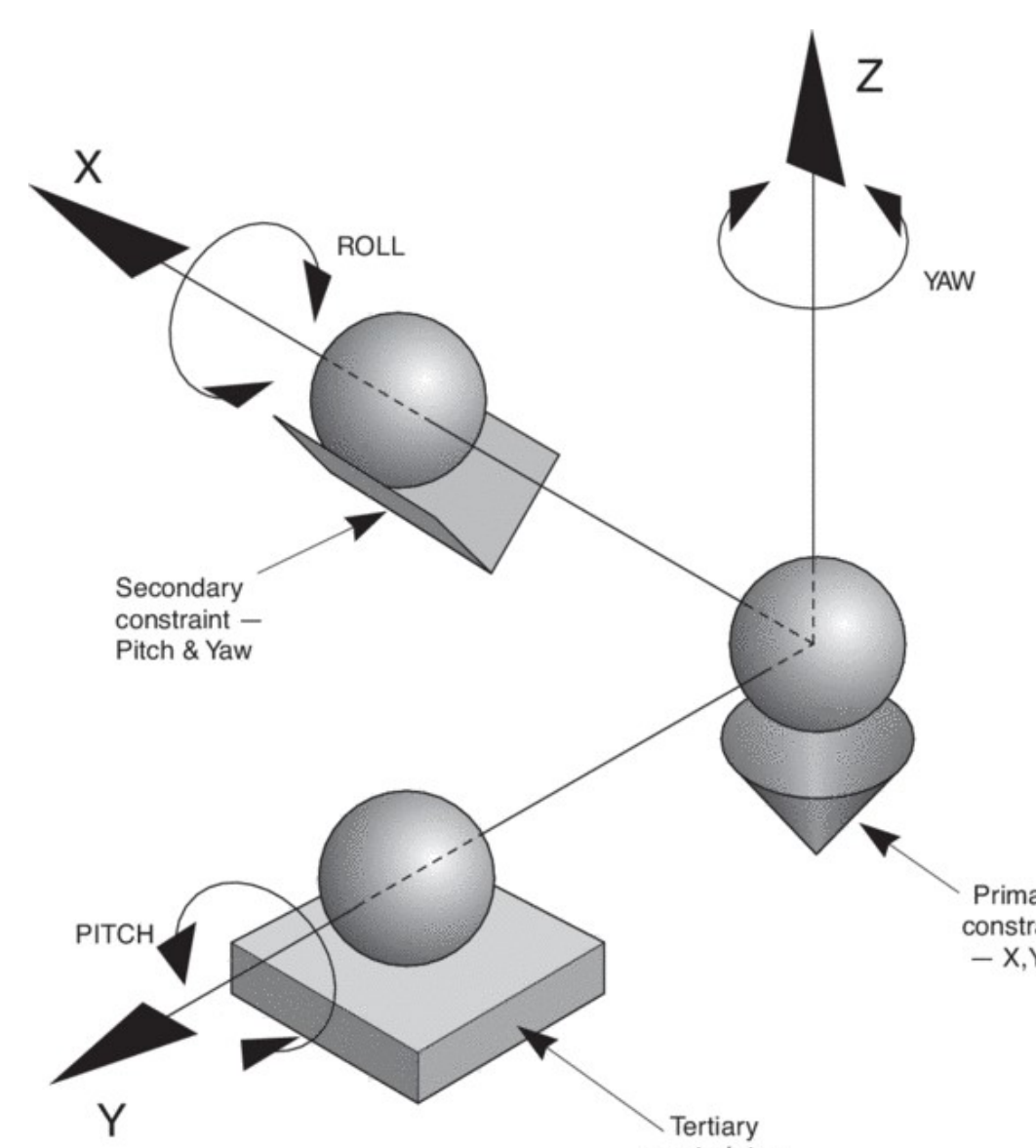


Fig. 3: Kelvin Coupling [1]

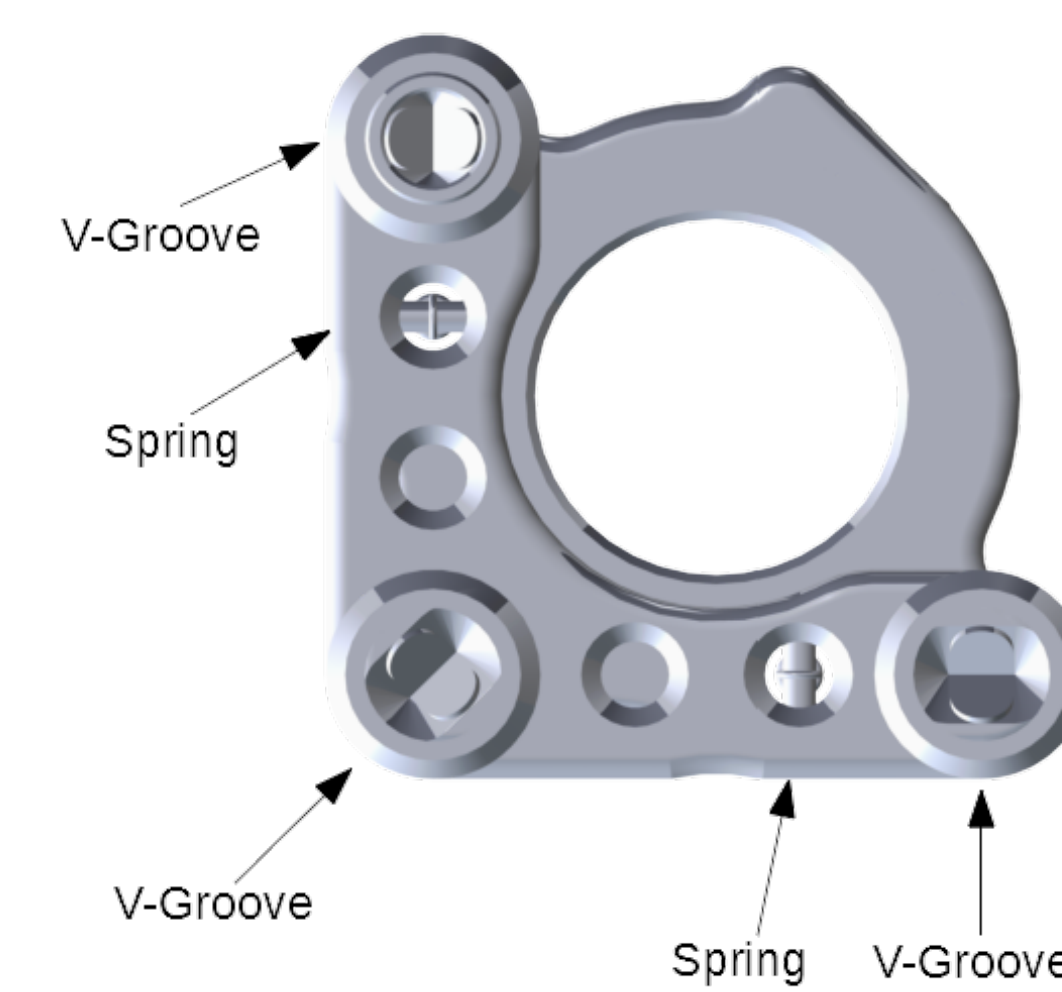


Fig. 4: Maxwell Coupling (Polaris-K1 Mount)

Mechanical Design for the RSNC

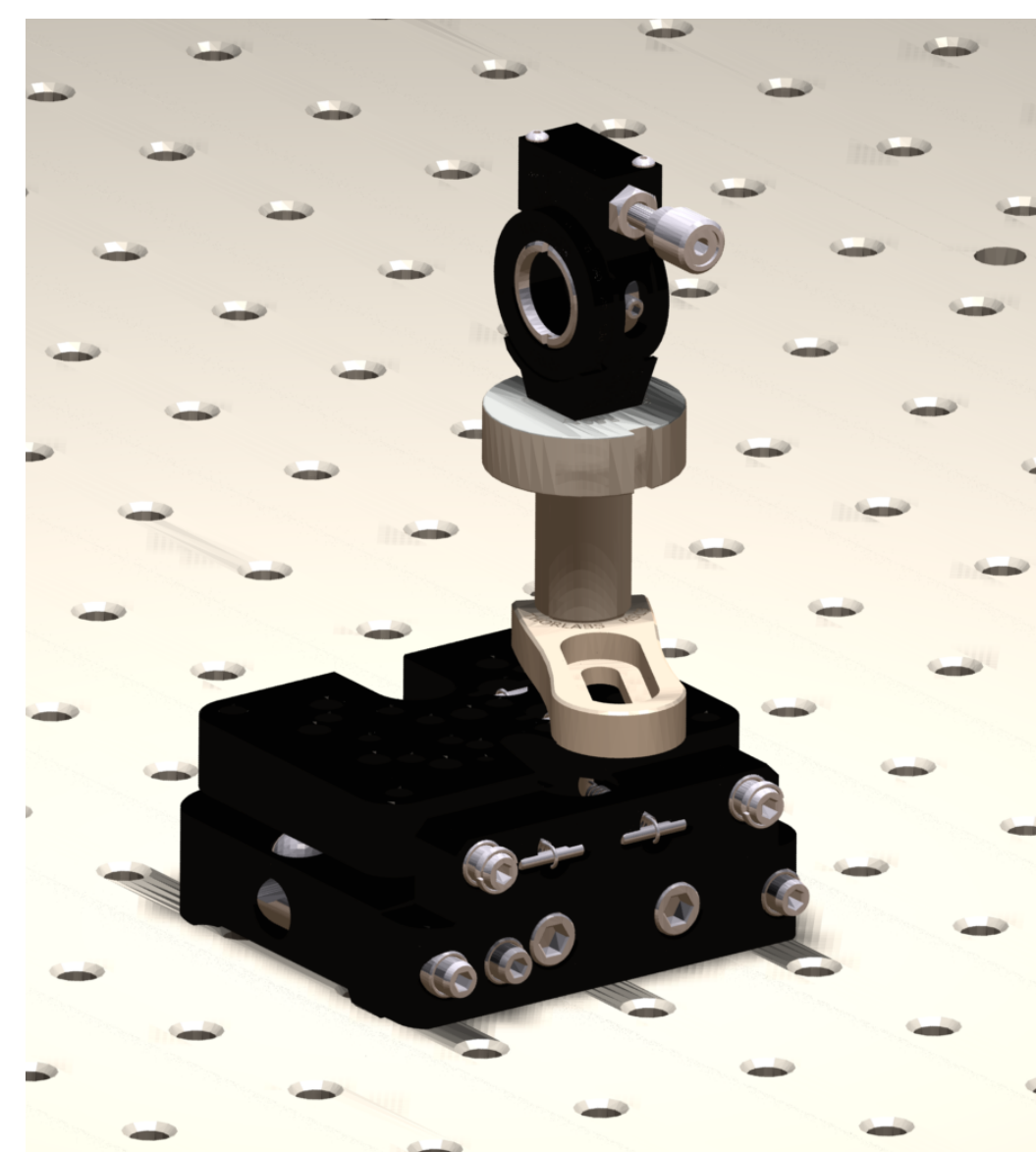


Fig. 5: Lyot Mask Mount

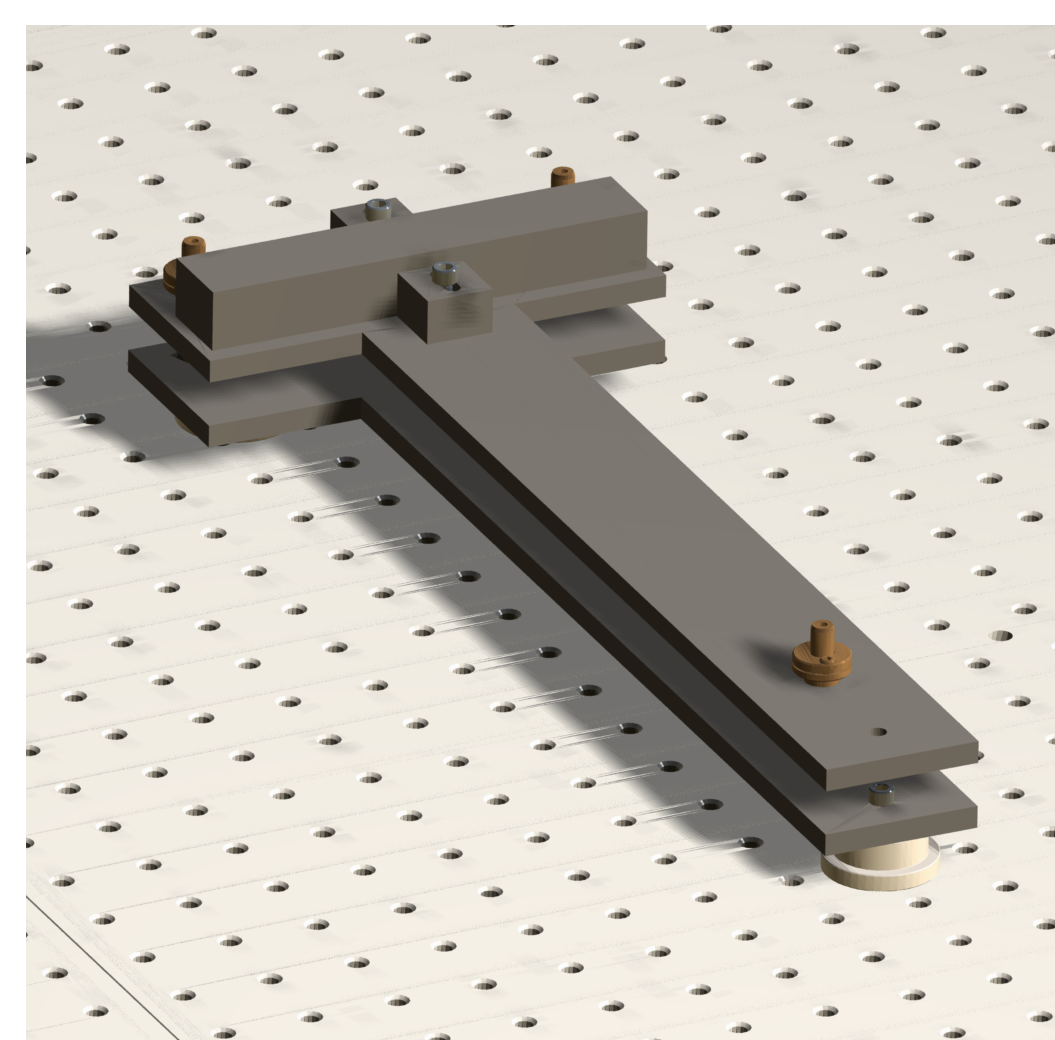


Fig. 6: Kinematic "T"-Mount

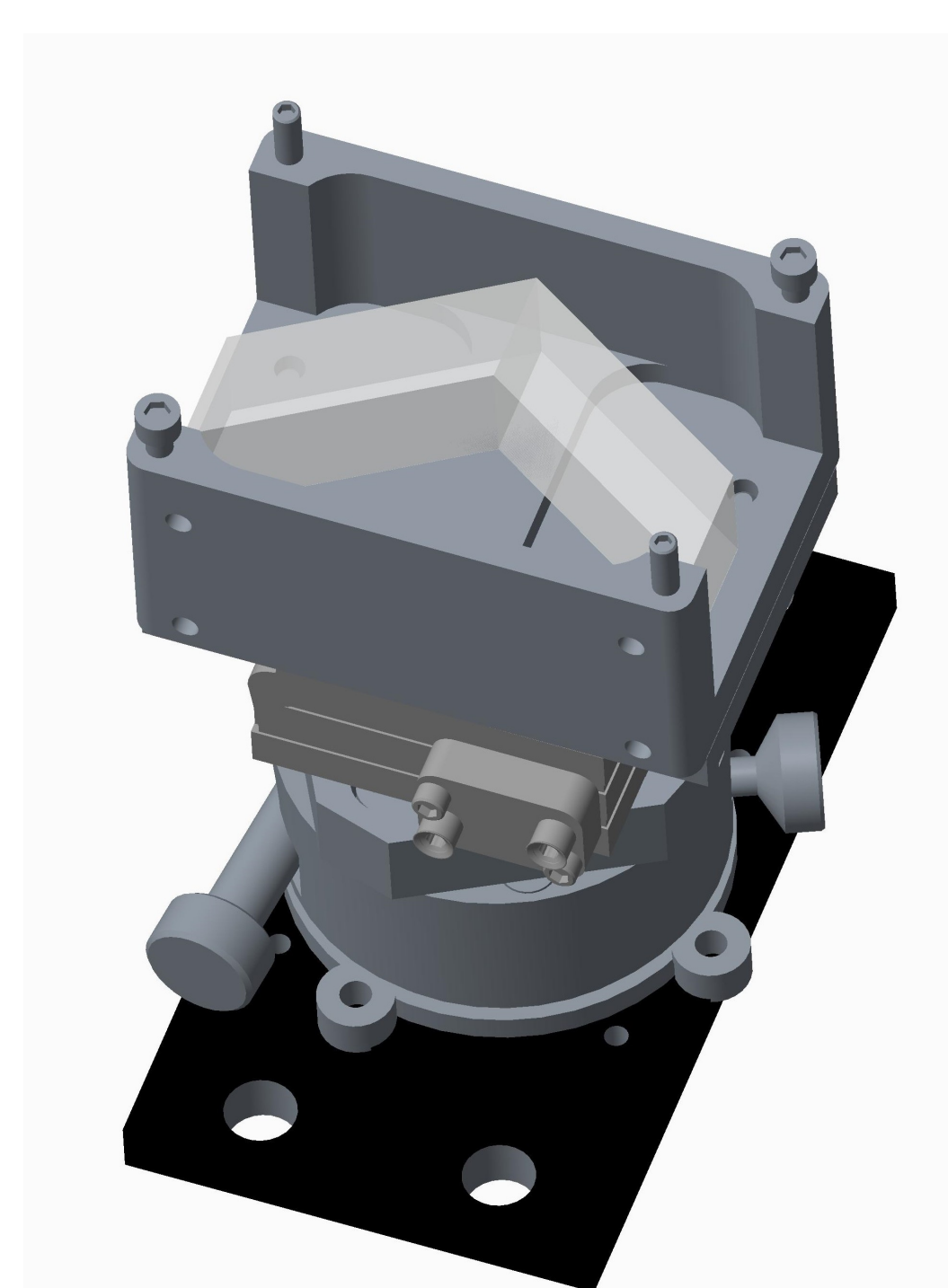


Fig. 7: Assembled Prisms

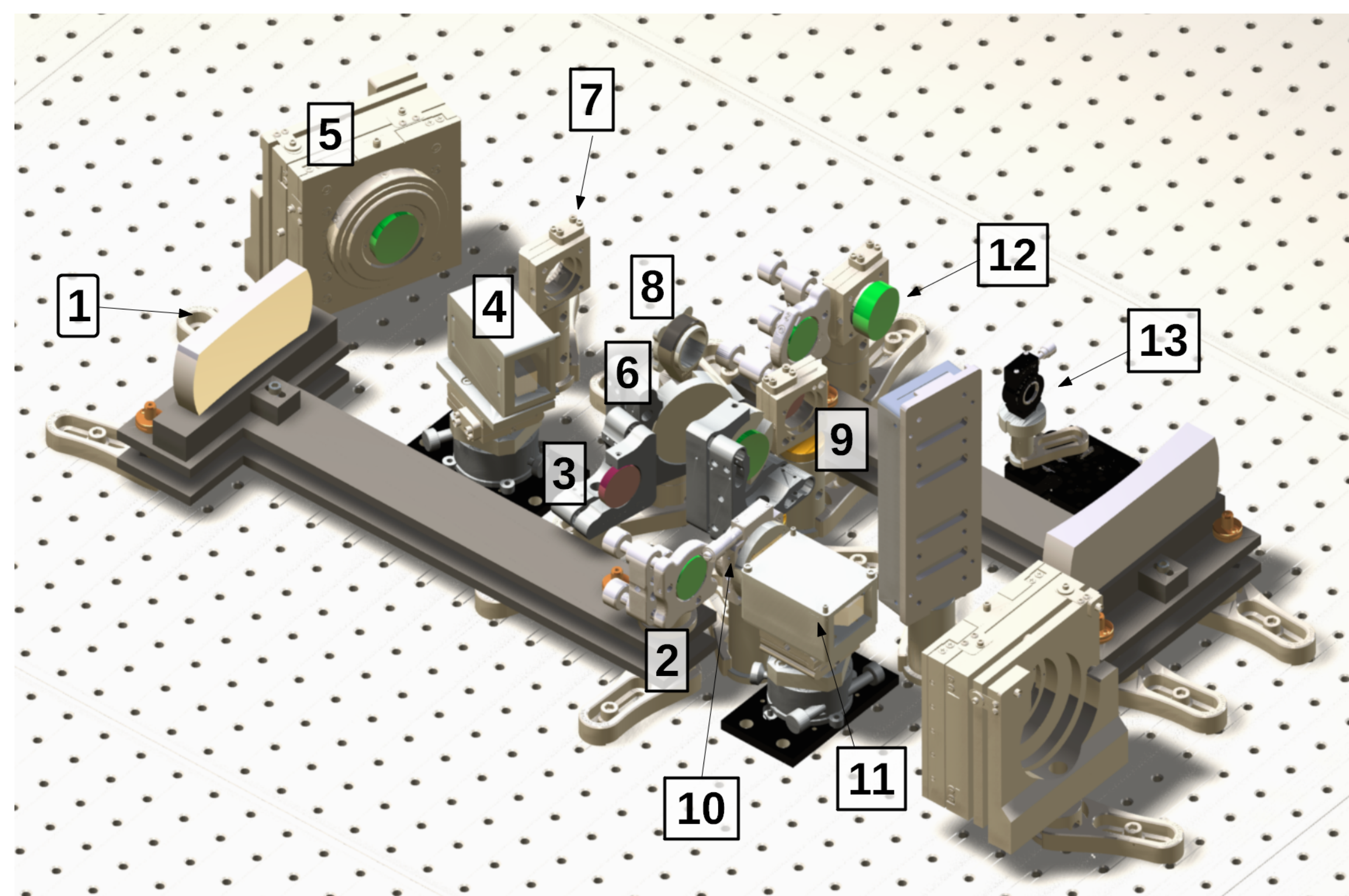


Fig. 8: Current RSNC model mounted to an optical breadboard

| # | Name | X (μm) | Y (μm) | Piston (μm) | Yaw (arcsec) | Pitch (arcsec) | Roll (arcsec) |
|----|-------------------------|---------------------|---------------------|--------------------------|--------------|----------------|---------------|
| 1 | Rectangular Mirror (x2) | - | 0.71 | - | - | 0.6 | 1.4 |
| 2 | Fold Mirror (x2) | - | - | 0.18 | 1.0 | 1.0 | - |
| 3 | BS1 | - | 0.71 | - | 3.8 | 3.8 | - |
| 4 | Fresnel Rhombs A | - | - | - | 3.0 | 4.5 | 4.5 |
| 5 | OAP1A/B | <1 | <1 | 10 | 5 | 5 | - |
| 6 | OAP2A/B | - | - | - | 2.6 | 2.6 | - |
| 7 | Delay Stage | - | - | 0.025 | 4.5 | 4.5 | - |
| 8 | Polarizer A | - | - | - | - | - | - |
| 9 | BS2 | - | - | - | 4.5 | 4.5 | - |
| 10 | Polarizer B | - | - | - | - | - | 300 |
| 11 | Fresnel Rhombs B | - | - | - | 3.0 | 4.5 | 4.5 |
| 12 | OAP3 | - | - | - | 4.5 | 4.5 | - |
| 13 | Lyot Mask | 254.0* | 146.5* | 146.5* | 1290* | 600* | 600 |

* per revolution

Fig. 9: Actuation Resolution for Optical Components

| # | Name | X (mm) | Y (mm) | Piston (mm) | Yaw ($^\circ$) | Pitch ($^\circ$) | Roll ($^\circ$) |
|----|-------------------------|--------|--------|-------------|------------------|--------------------|-------------------|
| 1 | Rectangular Mirror (x2) | - | 12.7 | - | - | 3 | 7 |
| 2 | Fold Mirror (x2) | - | - | 6 | 8 | 8 | - |
| 3 | BS1 | - | - | 12.7 | 19 | 19 | - |
| 4 | Fresnel Rhombs A | - | - | - | 360 | 5 | 5 |
| 5 | OAP1A/B | 3.2 | 3.2 | 6.4 | 5 | 5 | - |
| 6 | OAP2A/B | - | - | - | 13 | 13 | - |
| 7 | Delay Stage | - | - | 1.5 | 5 | 5 | - |
| 8 | Polarizer A | - | - | - | - | - | - |
| 9 | BS2 | - | - | - | 5 | 5 | - |
| 10 | Polarizer B | - | - | - | - | - | 14 |
| 11 | Fresnel Rhombs B | - | - | - | 360 | 5 | 5 |
| 12 | OAP3 | - | - | - | 5 | 5 | - |
| 13 | Lyot Mask | 3 | 3 | 3 | 10 | 7 | 14 |

Fig. 10: Actuation Range for Optical Components

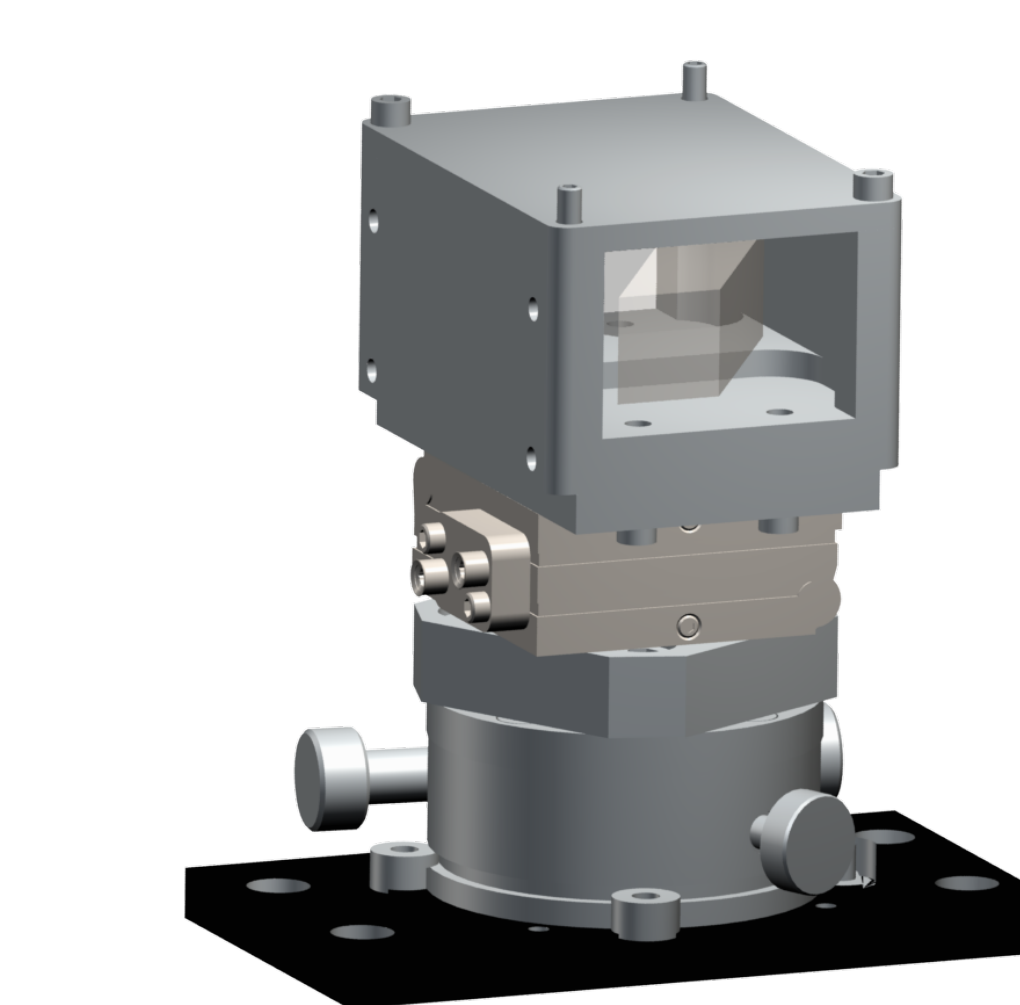


Fig. 11: Horizontal Assembly

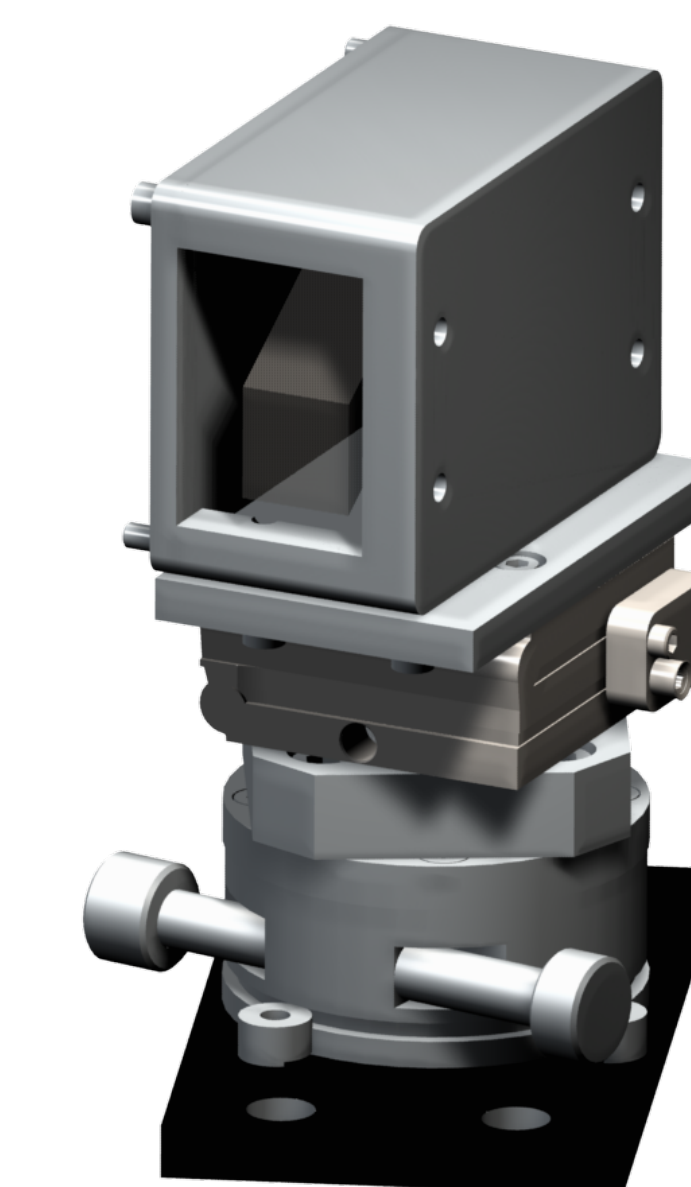


Fig. 12: Vertical Assembly

Fresnel rhombs use total internal reflections to change the polarization state of light by π . Custom multi-configurable mounts provide rotational control of the Fresnel rhombs about all three axes, and the enclosure protects the critical surfaces where total internal reflection occurs.

Alignment & Testing

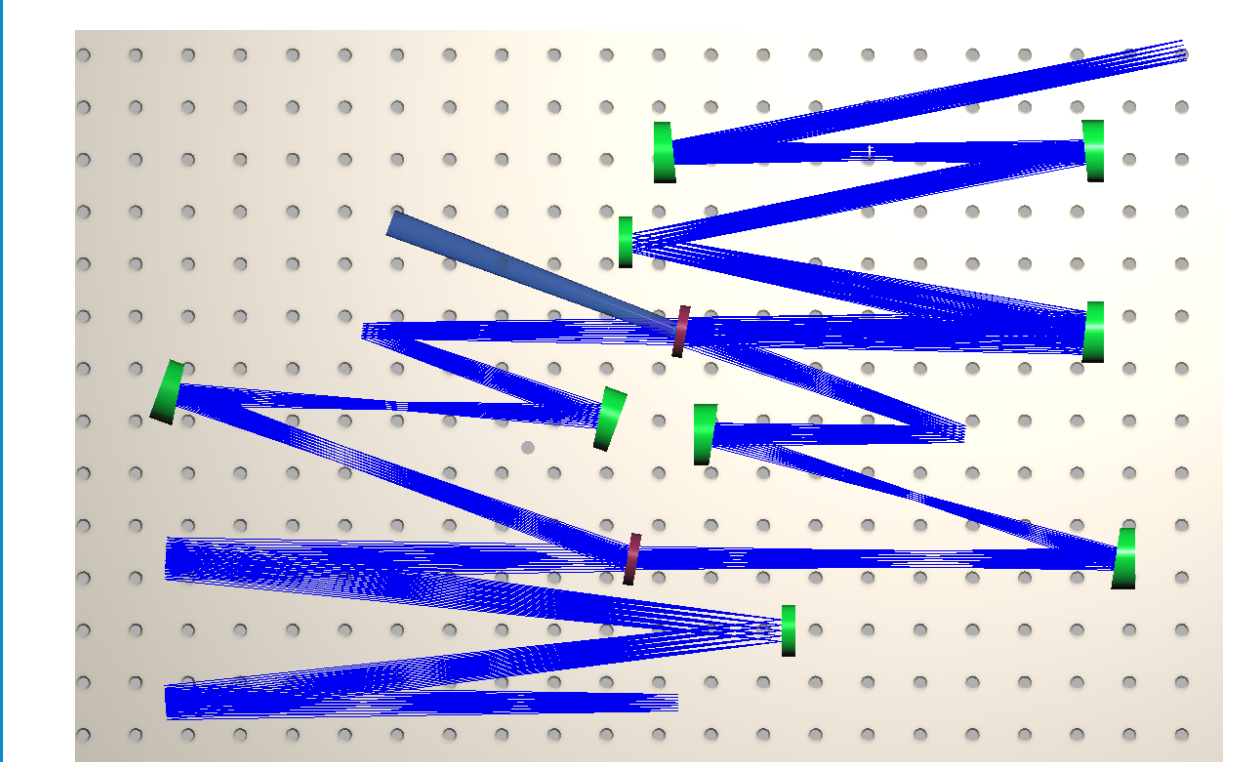


Fig. 13: Ideal Ray Trace

As part of the alignment process, optics 1 and 2 (Fig. 8) will be removed and aligned independently on their mount. Mounts are operated by hand and electronically: actuators vary from hex keys on micrometers to piezoelectric controllers.

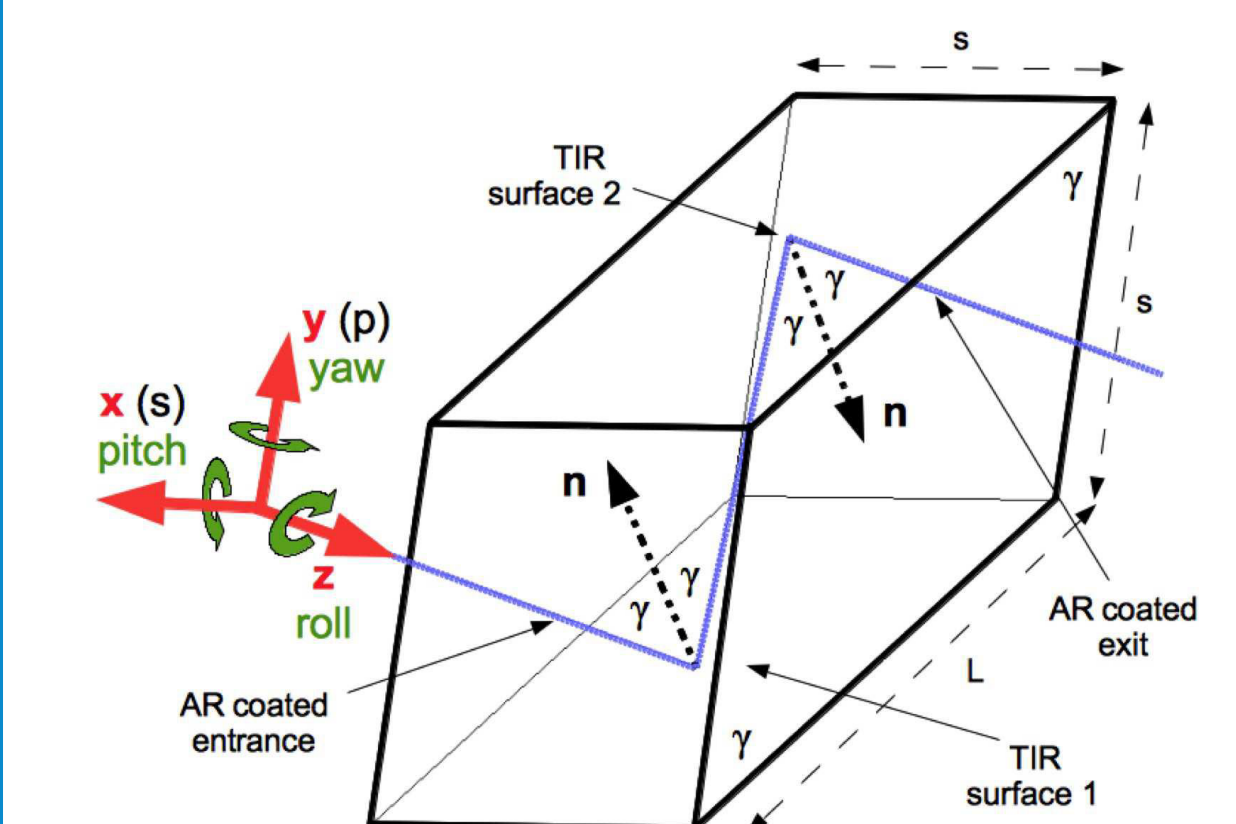


Fig. 14: Total Internal Reflection [2]

The Fresnel rhombs are sensitive to alignment errors because of the total internal reflection that occurs on their surfaces; therefore, they must have actuation capabilities in all rotational degrees of freedom.

Acknowledgements

A huge thank you is in place for everyone who helped make this project possible: to **Peter Petrone** who provided constant support and encouragement, to **Brian Kusnick** and **Matt Cosby** for their teamwork, to **Spencer Disque** for design collaboration, and to **CRESST II**. Special thanks to **Elisa Quintana** and **Tom Barclay** for the opportunity to gain experience with CubeSATS.

References

- [1] Newport Corporation. (n.d.). Optical Mirror Mount Technology Guide. Retrieved from <https://www.newport.com/n/optical-mirror-mount-technology-guide>
- [2] Hicks, Brian A., et al. "Demonstrating Broadband Billion-to-One Contrast with the Visible Nulling Coronagraph." *Techniques and Instrumentation for Detection of Exoplanets VII*, 2015, doi:10.1117/12.2189101.